[CANCER RESEARCH 64, 6603–6609, September 15, 2004]

G-Quartet Oligonucleotides: A New Class of Signal Transducer and Activator of Transcription 3 Inhibitors That Suppresses Growth of Prostate and Breast Tumors through Induction of Apoptosis

Naijie Jing,[1] Yidong Li,[1] Weijun Xiong,[1] Wei Sha,[1] Ling Jing,[2] and David J. Tweardy[1]

[1]*Department of Medicine, Section of Infectious Diseases, Baylor College of Medicine; and University of Texas Health Science Center, School of Public Health, Houston, Texas*

ABSTRACT

***Stat3* is a signaling molecular and oncogene activated frequently in many human malignancies including the majority of prostate, breast, and head and neck cancers; yet, no current chemotherapeutic approach has been implemented clinically that specifically targets Stat3. We recently developed G-rich oligodeoxynucleotides, which form intramolecular G-quartet structures (GQ-ODN), as a new class of Stat3 inhibitor. GQ-ODN targeted Stat3 protein directly inhibiting its ability to bind DNA. When delivered into cells using polyethyleneimine as vehicle, GQ-ODN blocked ligand-induced Stat3 activation and Stat3-mediated transcription of antiapoptotic genes. To establish the effectiveness of GQ-ODN as a potential new chemotherapeutic agent, we systemically administered GQ-ODN (T40214 or T40231) plus polyethyleneimine or polyethyleneimine alone (placebo) by tail-vein injection into nude mice with prostate and breast tumor xenografts. Whereas the mean volume of breast tumor xenografts in placebo-treated mice increased >7-fold over 18 days, xenografts in the GQ-ODN-treated mice remained unchanged. Similarly, whereas the mean volume of prostate tumor xenografts in placebo-treated mice increased 9-fold over 10 days, xenografts in GQ-ODN-treated mice increased by only 2-fold. Biochemical examination of tumors from GQ-ODN-treated mice demonstrated a significant reduction in Stat3 activation, levels of the antiapoptotic proteins Bcl-2 and Bcl-x_L, and an 8-fold increase in the number of apoptotic cells compared with the tumors of placebo-treated mice. Thus, GQ-ODN targeting Stat3 induces tumor cell apoptosis when delivered into tumor xenografts and represents a novel class of chemotherapeutic agents that holds promise for the systemic treatment of many forms of metastatic cancer.**

INTRODUCTION

Signal transducer and activator of transcription (STAT) proteins were originally discovered as latent cytoplasmic transcription factors (1). STAT proteins, including Stat1, 2, 3, 4, 5a, 5b, and 6 link to a variety of cellular and biological processes including proliferation, differentiation, apoptosis, host defense, and transformation (2–6). STAT proteins are localized within the cytoplasm of resting cells and become activated by tyrosine phosphorylation at their COOH-terminal end (Y705) after recruitment to activated receptor complexes. Tyrosine phosphorylation induces formation of dimers, which translocate to the nucleus, where they bind to DNA-response elements in the promoters of target genes and activate transcription (7).

Stat3, previously termed acute phase response factor (APRF; refs. 2, 8–10), is activated within cells by binding to the cell surface of >40 ligands; it also is constitutively activated in many human cancers (11–13) including 82% of prostate cancers (14), 69% of breast cancers (15), 82 to 100% of squamous cell carcinoma of head and neck (16), and 71% of nasopharyngeal carcinoma (17). Activated Stat3 upregulates the expressions of antiapoptosis proteins, such as Bcl-x_L and Mcl-1, thereby decreasing spontaneous apoptosis in cancer cells (18, 19). Targeting of Stat3 directly with agents, such as antisense oligonucleotides (20–22), a decoy oligonucleotide (23), or indirectly with Janus-activated kinase inhibitors, AG490 and JSI-124 (24, 25), demonstrated that Stat3 activation contributes to tumor cell growth and resistances to apoptosis, providing the strongest rationale for therapeutic approaches aimed at reducing levels or activity of Stat3 in cancers where it is activated.

Stat3, similar to all of the STAT proteins, is composed of several domains: a tetramerization domain, a coil-coil domain, a DNA-binding domain, a linker domain, an SH2 domain, a critical tyrosine reside (Y705), and a COOH-terminal transactivation domain. Resolution of the crystal structure of Stat3 revealed the structural basis for DNA-binding and dimer formation in sufficient detail to provide primary targets for novel drug development (26). One class of drug in early development as a novel agent targeting Stat3 is G-rich oligodeoxynucleotides (ODNs) that form G-quartet structures intracellularly (27).

G-rich DNA and RNA have the ability to form inter- and intramolecular four-stranded structures, referred to as G-quartets (28, 29). G-quartets arise from the association of four G-bases into a cyclic Hoogsteen H-bonding arrangement, and each G-base makes two H-bonds with its neighbor G-base (N1 to O6 and N2 to N7). G-quartets stack on top of each other to give rise to tetrad-helical structures. The stability of G-quartet structures depends on several factors: the presence of the monovalent cations, the concentration of the G-rich oligonucleotides present, and the sequence of the G-rich oligonucleotides under study. Potassium with the optimal size to interact within a G-octamer greatly promotes the formation of G-quartet structures and increases their stability. G-quartet oligodeoxynucleotides (GQ-ODNs) have been suggested to play a critical role in several biological processes including modulation of telomere activity (30), inhibition of human thrombin (31), HIV infection (32), HIV-1 integrase activity (33–35), human nuclear topoisomerase 1 activity (36), and DNA replication *in vitro* (37). On the basis of the structure and mechanism of Stat3 activation, G-quartet–forming oligonucleotides were developed recently to block Stat3 activity within cancer cells (27). GQ-ODNs directly target Stat3 protein and inhibit their ability to bind DNA thereby decreasing transcriptional activation of genes important for apoptosis resistance, such as *Bcl-x* and *Mcl-1*.

In the present report, we demonstrated that i.v. administration of GQ-ODNs dramatically reduces the growth in nude mice of xenografts of prostate and breast cancer cells in which Stat3 is constitutively activated. GQ-ODNs inhibited tumor cell growth by markedly enhancing tumor cell apoptosis and representing a promising agent for treatment of metastatic tumors in which Stat3 is constitutively activated.

MATERIALS AND METHODS

Materials. All of the G-rich ODNs including 5′-fluorescein-labeled ODN were synthesized by Midland Certified Reagent Company (Midland, TX) and used without additional chemical modifications. The human cell lines HepG2,

Received 12/24/03; revised 7/7/04; accepted 7/13/04.

Grant support: Department of Defense Award PC020407 and NIH Grants GM60153 and CA86430.

The costs of publication of this article were defrayed in part by the payment of page charges. This article must therefore be hereby marked *advertisement* in accordance with 18 U.S.C. Section 1734 solely to indicate this fact.

Requests for reprints: Naijie Jing, Department of Medicine, Section of Infectious Diseases, Baylor College of Medicine, Houston, TX. Phone: 713-798-3685; Fax: 713-798-8948; E-mail: njing@bcm.tmc.edu.

PC-3, and MDA-MB-468 were obtained from the American Type Culture Collection (Rockville, MD). Polyethylenimine (~25 kDa polymer, Sigma-Aldrich, Inc., St. Louis, MO) was generously provided by Dr. Charles Densmore (Baylor College of Medicine). Interleukin (IL) 6 and antibodies against Stat3, Stat1, Bcl-x_L, and Bcl-2 were purchased from Santa Cruz Biotechnology Biotechnology (Santa Cruz, CA). Antibody against caspase 3 was obtained from Cell Signaling Technology (Beverly, MA).

Assay of Inhibition by GQ-ODNs of Stat3 DNA-Binding Activity in Cancer Cells. GQ-ODN plus polyethyleneimine at a weight ratio of polyethyleneimine/ODN of 2:1 was added to cells ($5–7 \times 10^5$). After incubation for 3 hours, the cells were washed three times with fresh medium without polyethyleneimine/ODN and the incubation continued. After 6 to 72 hours, cells were incubated without or with IL-6 (25 ng/mL) at 37°C for 20 minutes before extraction and analysis by electrophoretic mobility shift assay. The cell extraction and electrophoretic mobility shift assay were performed as described previously (27). In some experiments, cells were scraped and harvested for isolation of nuclear proteins as described previously (38). Briefly, 50 μL of ice-cold Buffer A [10 mmol/L Tris-HCL (pH 9.), 2 mmol/L $MgCl_2$, 5 mmol/L KCl, 10% glycerol, 1 mmol/L EDTA, and 1 mmol/L DDT] plus 1% NP40 was added and the cells allowed to swell on ice for 15 minutes, then vortexed vigorously. The lysate was centrifuged at $700 \times g$ for 5 minutes at 4°C and the resulting nuclear pallet resuspended in 50 μL of cold buffer (20 mmol/L HEPES, 0.4 mol/L NaCl, 1 mmol/L EDTA, 1 mmol/L EGTA, and 1 mmol/L DDT). Nuclear proteins were extracted by vigorous shaking for 30 minutes at 4°C and cell debris pelleted by centrifugation at $18,000 \times g$ for 5 minutes at 4°C. Protein concentrations of whole-cell and nuclear extracts were measured by Bradford assay.

Statistical Docking Calculations. The structures of the designed G-quartet ODNs, such as T40214 and its analogues, were built up through modification of the nuclear magnetic resonance structure of GQ-ODN T30923 (39) and optimized under AMBER force field by INSIGHTII/DISCOVER. The optimization of the molecular structures proceeded as follows: (1) 100 steps of conjugate gradient energy minimization, (2) 1,000 steps of restrained MD equilibration with a time step of 0.33 fs at 1,000 K, (3) 1,000 steps of restrained MD equilibration with a time step of 0.1 fs at 300 K, and (4) 1,000 steps of conjugate gradient energy minimization. The intramolecular H-bonds of G-quartets were used as constraints for the molecular optimization.

We docked each GQ-ODN 1,000 times onto the available structure of the dimer of Stat3 SH2 (26) using the GRAMM docking program without placing any restrictions on binding sites. This program uses a geometry-based algorithm for predicting the structures of complexes between molecules of known structure. It can provide quantitative data related to the quality of the contact between the molecules. The intermolecular energy calculation relies on the well-established correlation and Fourier transformation techniques used in the field of pattern recognition. The distribution of H-bond formation between each Stat3/GQ-ODN complex was calculated and analyzed.

***In vivo* Delivery of Fluorescently Labeled GQ-ODN.** Fluorescent-labeled T40214 plus polyethyleneimine (each 2.5 mg/kg) was injected into the tail vein of male and female mice weighing ~20 g. Twenty-four hours after the infusion, the mice were sacrificed and tissue harvested and frozen. Frozen tissues were sectioned using cryostat microtome sections, lightly fixed, and viewed microscopically.

Tumor Xenograft Models. Athymic nude mice (Balb/*nu/nu*, 4 weeks old and weighing ~20 g obtained from Charles River Labs) were injected s.c. into the right (or left) flank with one million cancer cells (MDA-MD-468 or PC-3) in 200 μL of PBS. After tumors were established at 7 to 14 days postinjection, 16 nude mice with breast or prostate tumors were randomly assigned into three groups. Mice in group 1 ($n = 7$) served as placebo and received only polyethyleneimine (2.5 mg/kg), whereas mice in groups 2 and 3 ($n = 7$) received T40214 (5.0 mg/kg) plus polyethyleneimine (2.5 mg/kg) and T402314 (5.0 mg/kg) plus polyethyleneimine (2.5 mg/kg), respectively. Treatments, administered by tail-vein injection, and sizing of tumors occurred every 2 days. The unpaired two-sample *t* test, $\{t = (X_1 - X_2)/[S_p^2(1/n_1+1/n_2)]^{1/2}\}$, was used to determine differences in tumor sizes between the placebo and the drug-treated groups.

Immunoblotting. Tumor xenografts were harvested at the end of treatment period, cut into small pieces, homogenized on ice for 2 minutes, subjected to one round of freeze-thawing, and centrifuged (12,000 rpm for 2 min at 4°C). The supernatants were harvested, assayed for protein concentration by Bradford assay, and immunoblotted as described elsewhere (20).

Terminal Deoxynucleotidyl Transferase-Mediated dUTP-Biotin Nick End-Labeling Assay. The terminal deoxynucleotidyl transferase-mediated dUTP-biotin nick end-labeling (TUNEL) assay was performed as described by the manufacturer (Roche Applied Science, Indianapolis, IN). Briefly, prostate (or breast) tumors were harvested from mice within 24 hours of their last treatment. The paraffin-embedded tissues were pretreated using Xylene and EtOH, washed with PBS, and incubated with proteinase K working solution. TUNEL reaction mixture was prepared by adding 50 μL of enzyme solution into 450 μL of the labeling solution. TUNEL reaction mixture (50 μL) was placed on slides followed by 50 μL of 3,3′-diaminobenzidine substrate. Slides were incubated for 5 minute at 24°C, rinsed three times with PBS, dehydrated with xylene, and mounted under a glass coverslip.

RESULTS

Inhibition of Stat3 Activation by G-Quartet ODNs in Cancer Cells. Stat3 is expressed and constitutively activated in the prostate cancer cell line PC-3 and the breast cancer cell line MDA-MB-468 (14, 24). The GQ-ODN T40214 and a panel of related G-rich ODNs capable of forming G-quartets were mixed with polyethyleneimine, and each was examined for the ability to inhibit Stat3 activation in these cell lines (Fig. 1, *A–C*; Table 1). Each of the G-rich ODN demonstrated the ability to inhibit Stat3 DNA-binding activity when the concentration of ODN was increased from 7 to 285 μmol/L. T40214 and T40231 are the most potent inhibitors of Stat3 activation. Nonspecific ODNs incapable of forming the G-quartet structure demonstrated no activity against Stat3.

Structure–Activity Relationship between Stat3 and G-Quartet Inhibitors. T40214 was determined previously to form an intramolecular G-quartet structure composed of two G-quartets in the center and two G-C-G-C loop domains on the top and bottom with ~15Å

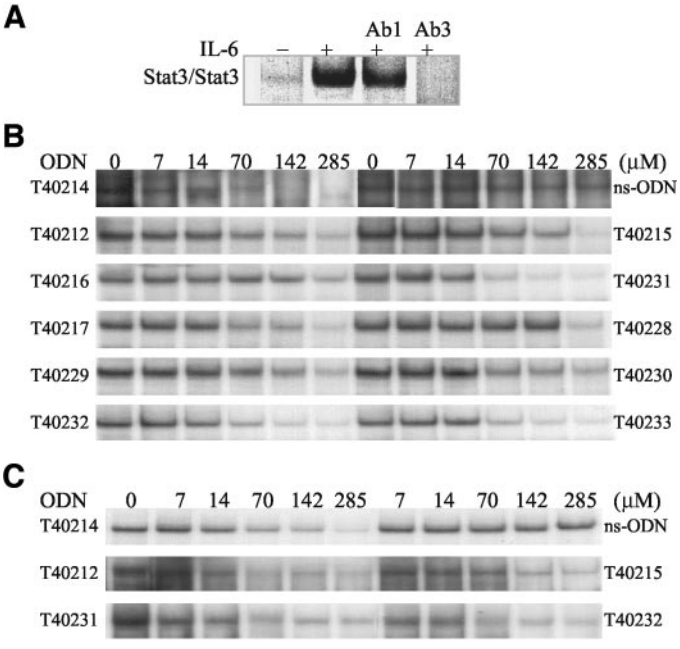

Fig. 1. Inhibition of Stat3 activation in prostate and breast cancer cells by GQ-ODN. *A*, Stat3 is activated constitutively and by IL-6 in PC-3 cells. Electrophoretic mobility shift assay was performed using extracts of PC-3 cells without (−) and with (+) stimulation with IL-6 (25 ng/ml); extracts were incubated without or with antibodies against Stat1 (*Ab1*) and Stat3 (*Ab3*). Electrophoretic mobility shift assay was performed using extracts of IL-6-stimulated PC-3 (*B*) and MDA-MB-468 cells (*C*) pretreated with each panel of ODN (see Table 1 for sequences). Cells were preincubated with the indicated ODN plus polyethyleneimine at the indicated concentration for 3 hours, washed, and incubated in fresh medium for 24 hours, and then stimulated with IL-6 (25 ng/ml) before extraction.

Table 1 *IC_{25}, IC_{50}, and IC_{75} of ODN for inhibition of IL-6–stimulated Stat3 activation in PC-3 cells and percentage of total H-bond formed between ODN and the region of Stat3 SH2 located between amino acid residues 638 and 650*

Compound	5′-sequence	IC_{25} (μM)	IC_{50} (μM)	IC_{75} (μM)	% H-bounds formed within Stat3 (aa 638–650)
Ns-ODN	TGCCGGATCCAAGAGCTACCA				
T40214	GGGCGGGCGGGCGGGC	2.5	5.0	24	35
T40212	GGGCGGGTGGGCGGGT	17	35	142	30
T40215	$(GGGGT)_4$	12	49	163	28
T40216	$(GGGGGT)_4$	30	202		
T40217	GGGGTGGGTGGGTGGGTT	35	64		27
T40228	GCGGGTGGGTGGGTGGGTCG	139	192	244	
T40229	TAGGGTGGGTGGGTGGGTAT	9	41	248	29
T40230	GTGGGTGGGTGGGTGGGTTG	11	43		28
T40231	GGTGGGTGGGTGGG	4.6	10	49	33
T40232	GGCGGGCGGGCGGG	10	26	62	32
T40233	GGGCGGGTGGGCGG	7.6	34	67	29

width and 15Å length (39, 40). T40214 and other GQ-ODNs destabilize Stat3 dimers by inserting between their SH2 domains. We proposed that GQ-ODNs interact in the region of the SH2 domain from amino acid residues 638 to 650 (ref. 27; Fig. 2*A*). To establish a structure–activity relationship between Stat3 and G-quartet inhibitors, we generated the G-quartet structure predicted to be formed by each G-rich ODN (Table 1) and randomly docked each of them onto the known structure of the dimer of Stat3 SH2 domains (26) 1,000 times. Analysis of the histogram of H-bonds formed at each residue within the Stat3 SH2 domain demonstrated that T40214 interacts with SH2 predominantly in the region from residues 638 to 650, as expected, with 35% of total H-bonds formed located in this region (Fig. 2*B*). The percentages of H-bonds formed within the region from residues 638 to 650 of Stat3 for other GQ-ODNs were listed in Table 1. Composite analysis of all of the histograms revealed that there is an inverse linear correlation between the percentage of GQ-ODN H-binding within this region of the Stat3 SH2 domain and the IC_{50} of inhibition of Stat3 DNA binding activity (Fig. 2*C*). Thus, these findings indicate that the higher the percentage of GQ-ODN H-bond formation within this region of Stat3 SH2, the greater its ability to inhibit Stat3 activation within cells.

GQ-ODN–Mediated Inhibition of Stat3 within Cells Is Selective for Stat3, Requires Polyethyleneimine, and Is Accompanied by Decreased Levels of Intranuclear Stat3 Phosphorylated on Y705 (Stat3-pY705). We demonstrated previously that GQ-ODN had 4-fold greater activity against Stat3 than Stat1 *in vitro* (27). To determine whether this selectively persisted or increased upon intracellular delivery, we preincubated HepG2 cells, in which both Stat3 and Stat1 are activated by IL-6, with T40214 (0–142 μmmol/L) for 72 hours before stimulation with IL-6. Preincubation of HepG2 cells with T40214/polyethyleneimine complex at 70 μmmol/L (or higher) nearly completely inhibited IL-6-mediated activation of Stat3, whereas activation of Stat1 was only mildly affected (Fig. 3, *A* and *C*) confirming the selectivity of GQ-ODN for Stat3 within cells. No inhibition of Stat3 DNA binding activity was observed when HepG2 cells were preincubated with T40214 in the absence of polyethyleneimine (Fig. 3*B*) confirming previous findings by us (40) that a vehicle is required for delivery of GQ-ODN into cells.

To determine whether GQ-ODNs also interfere with Stat3 activation and translocation into the nucleus, we examined levels of Stat3-pY705 within the nucleus of cells stimulated with IL-6 after GQ-ODN pretreatment. Levels of Stat3-pY705 were reduced from 50 to 70% in nuclei when the concentration of T40214 was increased from 3.5 to 142 μmmol/L (Fig. 4, lanes 4 to 7). polyethyleneimine alone as vehicle has no effect on Stat3 activation (Fig. 4, lane 3).

Delivery of G-Quartet ODN into Tumor Xenografts Results in Inhibition of Growth through Induction of Apoptosis. To determine whether GQ-ODNs can be administered to mice and delivered

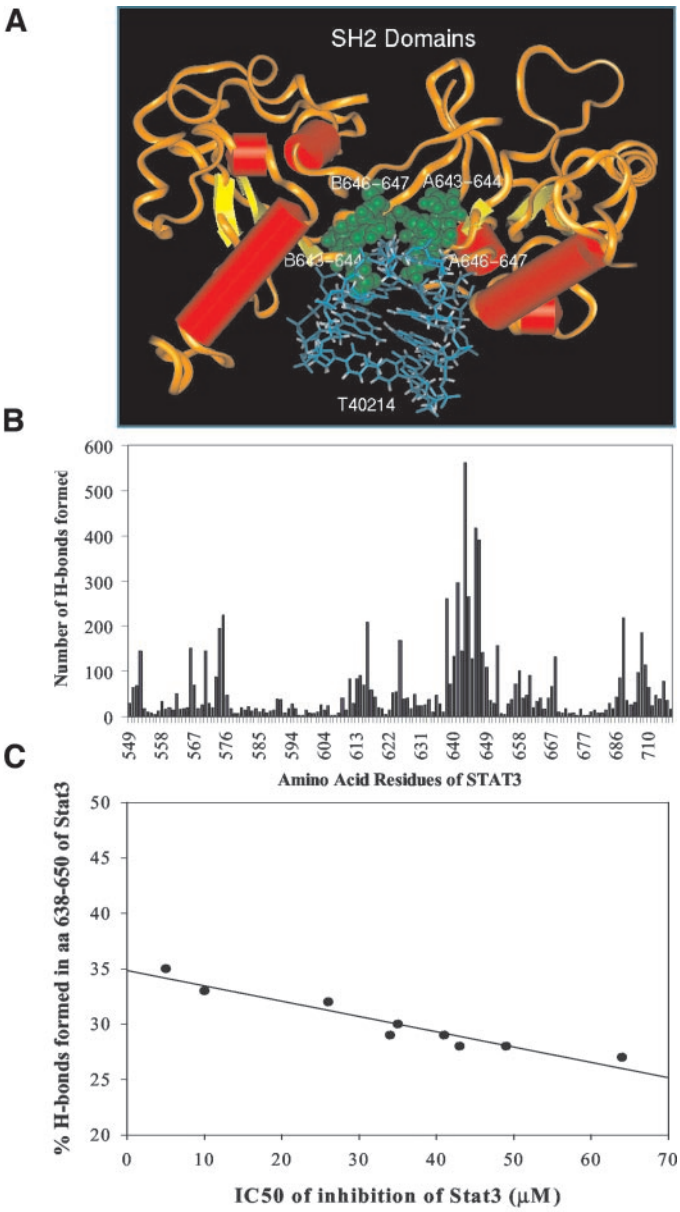

Fig. 2. Structure-activity relationship of GQ-ODNs. *A*, model of T40214 bound to dimers of Stat3 SH2 showing T40214 (*blue wire model*) interacting with residues Q643, Q644, N646, and N647 of Stat3 dimer (*green space-filling model*). *B*, histogram of the distribution of all H-bonds formed between T40214 and the SH2 domain of Stat3 in 1,000 computer-simulated dockings. *C*, plot demonstrating the relationship between the percentage of GQ-ODN H-bonding localized from residues 638 to 650 and its IC_{50} against Stat3 (Table 1; $r^2 = 0.91$; $P < 0.001$).

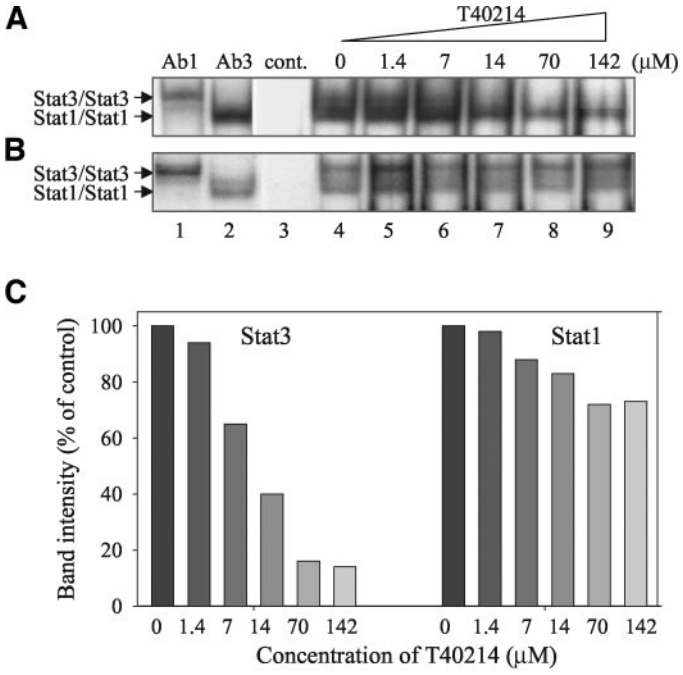

Fig. 3. GQ-ODN selectively targets Stat3 within cells, and its delivery requires polyethyleneimine. Electrophoretic mobility shift assay of extracts of HepG2 cells stimulated with IL-6 (25 ng/ml) 72 hours after preincubation of cells with T40214 at the indicated concentrations complexed with (*A*) or without (*B*) polyethyleneimine. Extracts were incubated with antibodies against Stat1 (*Ab1*; *Lane 1*) or Stat3 (*Ab3*; *Lane 2*) to confirm the composition of the homodimer bands. *C*, Intensity of the homodimer bands in *lanes 4* through 9 of T40214 with polyethyleneimine (*A*) were measured by densitometry and plotted as a percentage of the band in the untreated lane (0 μmol/L; *lane 4*).

into tumor xenografts, we injected fluorescein-labeled T40214 plus polyethyleneimine (each at 2.5 mg/kg) into the tail veins of nude mice with established tumor xenografts. Microscopic examination of xenografts 24 hours after injection demonstrated diffuse fluorescent staining within tumor cells (Fig. 5*A*) indicating that GQ-ODN enters and accumulates within tumor cells.

The two most active GQ-ODNs, T40214 and T40231 (Fig. 5*B*), were selected from among the designed GQ-ODNs to assess if GQ-ODN uptake is accompanied by inhibition of tumor growth. Nude mice were injected s.c. with MDA-MB-468 or PC3, both of which demonstrate constitutive Stat3 activity, and i.v. treated every other day after tumors were established (Fig. 5, *C* and *D*). The drug treatment groups received T40214 or T40231 (5.0 mg/kg) plus polyethyleneimine (2.5 mg/kg), and the placebo groups each received polyethyleneimine (2.5 mg/kg) alone by tail-vein injection. The mean size of the breast tumor xenografts of placebo-treated mice increased from 7- to 12-fold, whereas the mean sizes of both T40214 and T40231-treated mice remained unchanged (Fig. 5*C*). The growth rate of placebo-treated breast tumors ranged from 11% to 15%/day, and those of T40214 and T40231-treated breast tumors were −0.4%/day ($P = 0.001$) and 0.6%/day ($P = 0.001$), respectively. The mean size of the prostate tumor xenografts of placebo-treated mice increased 9- to 10-fold, whereas the mean sizes of T40214-treated and T40231-treated mice increased only 2.2- and 2.6-fold, respectively (Fig. 5*D*). The growth rate of placebo-treated prostate tumors ranged from 21% to 23%/day, whereas the growth of T40214- and T40231-treated prostate tumors was 9.1%/day ($P = 0.001$) and 8.8%/day ($P = 0.001$), respectively.

To gain insight into the mechanism of inhibition of tumor growth by GQ-ODN, we harvested the prostate tumor xenografts from placebo-treated and drug-treated mice after five treatments and extracted proteins to assess for levels of Stat3-pY705, Bcl-x_L, Bcl-2, and activated caspase 3 protein. Levels of Stat3-pY705, Bcl-x_L, and Bcl-2 were decreased by 9-, 4.3-, and 10-fold, respectively, in the tumors from drug-treated animals compared with tumors from placebo-treated mice. These changes were accompanied by a 3-fold increase in caspase 3 cleavage products in the tumors from drug-treated animals compared with tumors from placebo-treated mice (Fig. 6*A*). We have harvested the 4 tumor samples from placebo-treated mice and 3 tumor samples from drug-treated mice and then performed TUNEL assay on the samples. TUNEL staining was performed on 4 tumor samples from placebo-treated mice and 3 tumor samples from drug-treated mice to assess if GQ-ODN treatment increased tumor cell apoptosis. The percentage of apoptotic cells was increased nearly 8-fold in the tumors of drug-treated mice (83.6 ± 1.0%) compared with the tumors of placebo-treated mice (11.2 ± 10.1%; $P < 0.001$; Fig. 6*B*).

DISCUSSION

Mounting evidence from cell culture, whole animals, and patient samples indicates that Stat3 is a critical mediator of oncogenic signaling that is activated in many human malignancies (17). This evidence provides a strong rationale for developing agents that target Stat3 for treatment of cancers in which constitutive Stat3 activation plays a critical role. Currently, no chemotherapeutic approach has been implemented that targets Stat3. We recently developed G-rich oligodeoxynucleotides, which form intramolecular G-quartet structures (GQ-ODNs), as a new class of Stat3 inhibitor; GQ-ODNs were shown to target Stat3 dimers predominantly in the regions of their SH2 domains resulting in their destabilization and reduced ability to bind DNA *in vitro* (27). In studies reported here, we demonstrate that when delivered into cells using polyethyleneimine as vehicle, GQ-ODNs blocked ligand-induced Stat3 activation. We determined that the region within the SH2 dimer domains predominantly bound by

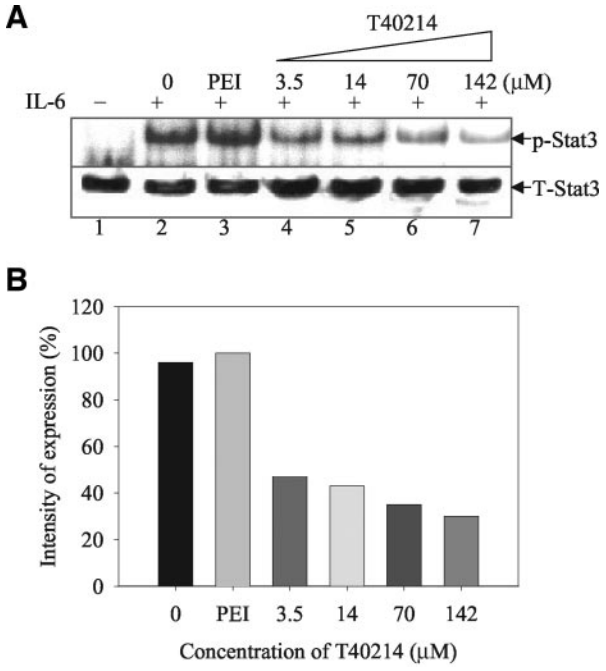

Fig. 4. GQ-ODN inhibit IL-6-mediated increase in intranuclear phosphorylated Stat3. *A*, immunoblot of nuclear extracts of HepG2 cells preincubated with media (*0*), polyethyleneimine alone (*PEI*), or T40214 at the indicated concentrations for 3 hours. Cells were then washed and incubated in medium alone for 24 hours before stimulation with IL-6 (25 ng/mL); nuclear extracts were separated by SDS-PAGE and immunoblotted with antiphosphotyrosine antibody (pY705; *top*) or Stat3 monoclonal antibody (T-Stat3, *bottom*). *B*, The p-Stat3 bands were quantitated by densitometry and plotted as the percentage of the polyethyleneimine-pretreated lane (*lane 3*).

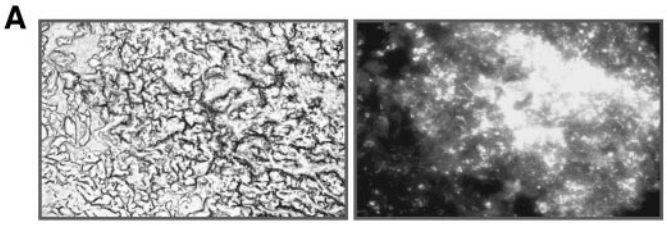

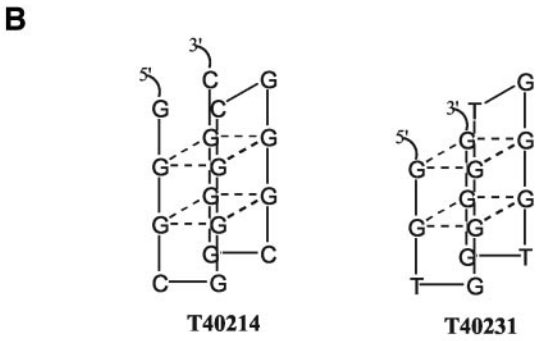

Fig. 5. GQ-ODN is successfully delivered into tumor xenografts and inhibits their growth. *A*, light microscopic (*left*) and fluorescent microscopic (*right*) photomicrographs (each ×400 magnification) of a tumor xenograft harvested from a nude mouse 24 hours after tail-vein injection with fluorescein-labeled T40214/polyethyleneimine complex (each at 2.5 mg/kg), showing the uptake of T40214 within tumor cells. *B*, the models of T40214 and T40231 structures. Breast (*C*) and prostate (*D*) cancer cells xenograft volumes were measured at the start of therapy and every other day in mice treated with T40214/polyethyleneimine complex (○) or with polyethyleneimine alone (●; *top*) or with T40231/polyethyleneimine complex or with polyethyleneimine alone (*bottom*). Data plotted are fold increase in tumor volume of each group; *bars*, ±SE.

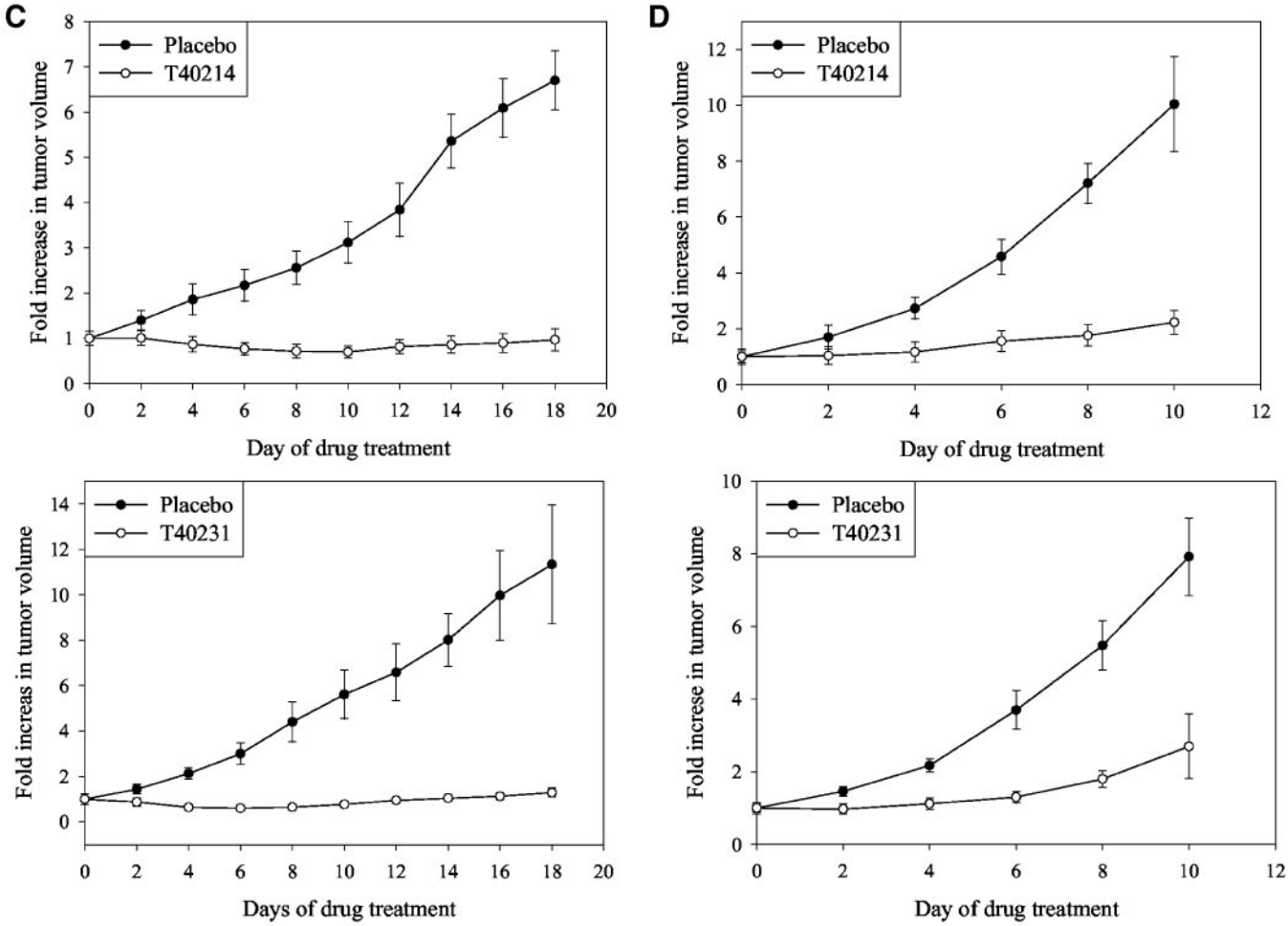

GQ-ODN was located between residues 638 and 650, a region critically involved in Stat3 dimerization. Importantly, we established a linear structure-activity relationship that directly correlates the ability of a GQ-ODN to bind to this region of Stat3 SH2 and its ability to inhibit Stat3 activation within cells, which is an important step toward optimizing the design GQ-ODN inhibitors of Stat3. Furthermore, intravenous administration of GQ-ODNs plus polyethyleneimine blocked the growth of breast and prostate tumor xenografts in nude mice. This effect was accompanied by marked reductions in levels of Stat3 activation and Bcl-2 and Bcl-x_L protein and a striking increase

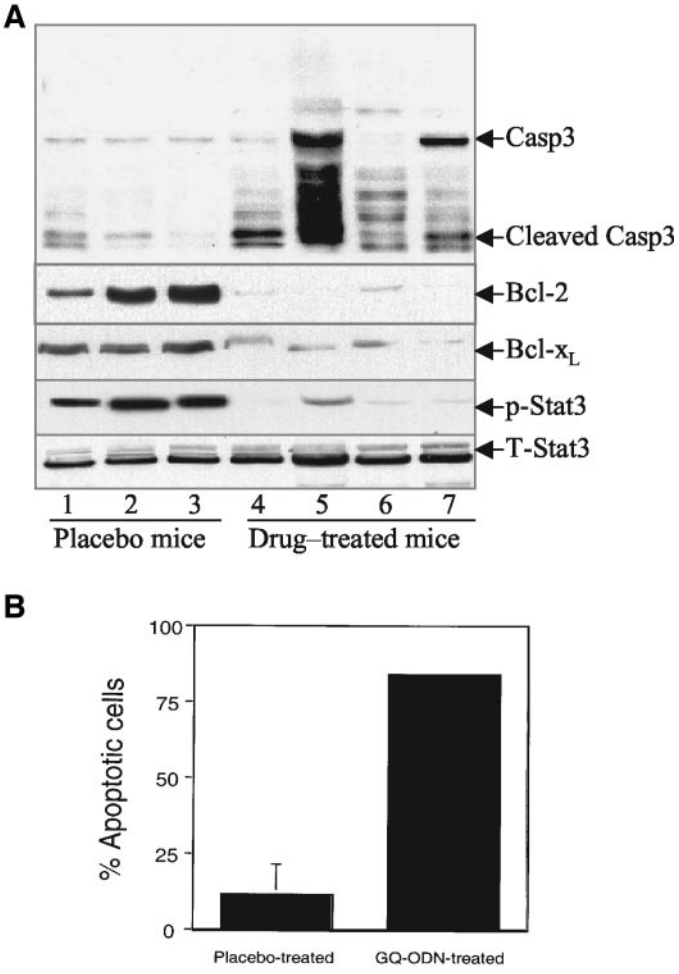

Fig. 6. Effect of G-quartet ODN T40214 on apoptosis and levels of apoptosis-related proteins in tumor xenografts. *A*, Proteins were extracted from tumor xenografts obtained from 3 placebo-treated mice (*lanes 1* to *3*) and from 4 drug-treated mice (*lanes 4* to *7*), separated by SDS-PAGE, and immunoblotted with the antibodies indicated. Each lane was loaded an equal amount of the total *Stat3 (T-Stat3*) protein as a control. *B*, percentage of apoptotic cells within prostate tumor xenografts assessed by TUNEL staining. Two hundred cells within TUNEL stained sections of prostate tumor xenografts removed on day 10 from placebo-treated mice ($n = 4$) and GQ-ODN-treated mice ($n = 3$) were examined at ×400 magnification. Data presented are the mean; *bars*, ±SD; $P < 0.001$.

in tumor cell apoptosis. Thus, GQ-ODNs, which target Stat3 and induce apoptosis within tumor xenografts after intravenous administration, represent a novel cancer chemotherapeutic approach that holds promise for the systemic treatment of many forms of metastatic cancer.

Our previous studies showed that the G-quartet structure of G-rich ODN is essential for the inhibition of Stat3 DNA-binding activity *in vitro* (27). The G-quartet structure of T40214 closely resembles a perfect cylinder 15 Å in width and length. This conformation increases the thermal stability of the structures, reduces the capacity of ODN to form molecular aggregates, and increases the probability that each GQ-ODN will target Stat3 homodimer in cells. The finding that T40214-mediated inhibition of ligand-induced Stat3 activation within cells persisted for 72 hours after GQ-ODN exposure can be attributed, in part, to this compact configuration, which contributes to its thermal stability and resistance to nuclease digestion. The intramolecular G-quartet structure prevents single-strand endonucleases from accessing their cleavage sites (41).

Effective delivery of GQ-ODNs into cancer cells is a key factor for success of inhibitors that target oncogenic signaling intermediates. On the basis of the property of potassium-dependent formation of G-quartet structure, a novel intracellular delivery system has been developed for GQ-ODNs (40). Using the novel delivery system, GQ-ODNs were delivered efficiently into the cytoplasm and nucleus of cells. The results reported here showed that GQ-ODNs penetrated poorly into cells without vehicle as evidenced by low drug activity, whereas use of an effective intracellular delivery system such as polyethyleneimine increased the drug activity of GQ-ODNs in cancer cells (Fig. 3, *A* and *B*). When G-rich ODNs form intramolecular G-quartet structures within the cytoplasm, they are able to diffuse freely through pores into the nucleus, bind to Stat3, and block the transcription of Stat3-regulated genes (Fig. 4; ref. 27).

Because of the important role that STAT proteins play in signaling within the immune system (Stat1, 2, 4, 5A, 5B, and 6) and in negative regulation of proliferation (Stat1; ref. 42), it is highly desirable that an agent targeting Stat3 not have activity against other STAT proteins to avoid problems with immunosuppression and inadvertent stimulation of tumor cell growth. On the basis of their structures (14, 43), the ligand-receptor pairs that lead to their activation (1) and the phosphotyrosine sites that lead to their recruitment and activation (44), the STAT protein family member that most closely resembles Stat3 is Stat1. Stat3 and Stat1 share >50% amino acid sequence homology in the region of the SH2 domain (13). Therefore, to address the issue of specificity of GQ-ODN inhibition, we focused on Stat1. In previous studies, we demonstrated that the IC_{50} of T40214 for the inhibition of Stat3 DNA-binding activity *in vitro* was 4-fold less than for its inhibition of Stat1 DNA-binding activity (27). Here, we demonstrated that the specificity of T40214 for Stat3 *versus* Stat1 extends *in vivo*. The concentration of T40214 that inhibited 50% of Stat3 activation after preincubation of T40214 in cells was ~10 μmol/L (Fig. 3*C*), whereas 50% inhibition of Stat1 under the same conditions could not be achieved with concentrations of T40214 up to142 μmol/L. The basis for this selectivity was explained, in part, by the analysis of histograms, which were generated by docking the structure of T40214 onto the structures of Stat3β and Stat1 homodimers 2,000 times without setting any binding site restrictions (26). These studies demonstrated that interactions of GQ-ODN with Stat3 were concentrated within the SH2 and DNA-binding domains; in contrast, interactions of GQ-ODN with Stat1 were distributed more broadly over the whole structure of Stat1.

Intravenous administration of GQ-ODN plus polyethyleneimine was well tolerated by mice at the dose used in this study. Detailed toxicity studies of T40214 and T40231 are in progress; however, toxicity studies of GQ-ODN T30177, an analogue of T40214 that inhibits HIV-1 integrase, has been performed previously (45). T30177 did not induce genetic mutations in three assays, the *Ames*/*Salmonella* mutagenesis assay, the Chinese hamster ovary/hypoxanthine-guanine phosphoribosyltransferase mammalian cell mutagenesis assay, and the mouse micronucleus assay. Acute toxicity studies in mice revealed an LD_{50} for T30177 of 1.5g/kg body weight; chronic toxicity studies in mice after multiple doses did not cause delayed mortality or changes in serum chemistry, hematologic parameters, or organ histology until the dose of T30177 reached 600 mg/kg, 120 times the dose (5 mg/kg) used in our studies.

The results of *in vivo* drug testing revealed that GQ-ODN T40214 dramatically suppressed the growth of xenografts of prostate and breast cancer cells in which Stat3 is constitutively activated. GQ-ODN T40214 markedly decreased the level of phosphorylated Stat3 in tumor xenografts; this decrease was associated with decreased levels of Bcl-2 and Bcl-x_L protein. Bcl-2 and Bcl-x_L are antiapoptosis proteins that have ion channel activity, which inhibit the release from mitochondria of cytochrome C (46, 47). Reduced levels of Bcl-2 and Bcl-x_L in tumor xenografts would result in increased release of cytochrome C resulting in activation of the caspase cascade, which

includes caspase 3, leading to cell apoptosis. There was a striking increase in caspase 3 cleavage products in the tumors of T40214-treated animals that was accompanied by an increase in tumor cell apoptosis of similar magnitude. Our results indicate that GQ-ODNs such as T40214 block tumor xenograft growth by targeting Stat3 and inhibiting its phosphorylation, which blocks the transcription of the antiapoptosis proteins and triggers the apoptosis of cancer cells. Thus, GQ-ODNs represent a novel and potentially promising class of drug for treatment of metastatic tumors in which Stat3 is constitutively activated as either a single agent or part of a combination regimen.

REFERENCES

1. Darnell Jr JE. STATs and gene regulation. Science 1997;277:1630–5.
2. Zhong Z, Wen Z, Darnell Jr JE. Stat3: a STAT family member activated by tyrosine phosphorylation in response to epidermal growth factor and interleukin-6. Science 1994;264:95–8.
3. Bromberg JF, Horvath CM, Wen Z, Schreiber RD, Dannell Jr JE. Transcriptionally active Stat1 is required for the antiproliferative effects of both interferon alpha and interferon gamma. Proc Natl Acad Sci USA 1996;93:7673–8.
4. Fukada T, Hibi M, Yamanaka Y, et al. Two signals are necessary for cell proliferation induced by a cytokine receptor gp130: involvement of STAT3 in anti-apoptosis. Immunity 1996;5:449–60.
5. Planas AM, Berruezo M, Justicia C, Barron S, Ferrer I. Stat3 is present in the developing and adult rat cerebellum and participates in the formation of transcription complexes binding DNA at the sis-inducible element. J Neurochem 1997;68:1345–51.
6. Takeda K, Noguchi K, Shi W, et al. Targeted disruption of the mouse Stat3 gene leads to early embryonic lethality. Proc Natl Acad Sci USA 1997;94:3801–4.
7. Bromberg J, Darnell JE. The role of STATs in transcriptional control and their impact on cellular function. Oncogene 2000;19:2468–73.
8. Wegenka UM, Lutticken C, Buschmann J, et al. The interleukin-6-activated acute-phase response factor is antigenically and functionally related to members of the signal transducer and activator of transcription (STAT) family. Mol Cell Biol 1994; 14:3186–96.
9. Lutticken C, Wegenka UM, Yuan J, et al. Association of transcription factor APRF and protein kinase jak 1 with the interleukin-6 signal transducer gp130. Science 1994;263:89–92.
10. Raz R, Durbin JE, Levy DE. Acute phage response factor and additional member of the interferon-stimulated gene factor 3 family integrate diverse signals from cytokines, interferons, and growth factor. J Biol Chem 1994;269:24391–5.
11. Bowman T, Garcia R, Turkson J, Jove R. STATs in oncogenesis. Oncogene 2000; 19:2474–88.
12. Bromber, J.F. Activation of STAT proteins and growth control. BioEssay 2001;23: 161–9.
13. Buettner R, Mora LB, Jove R. Activated STAT signaling in human tumor provides novel molecular targets for therapeutic intervention. Clin Cancer Res 2002;8:945–54.
14. Mora LB, Buettner R, Seigne J, et al. Constitutive activation of Stat3 in human prostate tumors and cell lines: direct inhibition of Stat3 signaling induces apoptosis of prostate cancer cells. Cancer Res 2002;62:6659–66.
15. Dolled-Filhart M, Camp RL, Kowalski DP, Smith BL, Rimm DL. Tissue microarray analysis of signal transducers and activator of transcription 3 and phospho-state 3 (Tyr705) in node-negative breast cancer shows nuclear localization is associated with a better prognosis. Clinical Cancer Res 2003;9:594–600.
16. Nagpal JK, Mishra R, Das BR. Activation of Stat3 as one of early events in tobacco chewing-mediated oral carcinogenesis. Amecrican Cancer Sociaty 94:2393–400.
17. Hsiao J-R, Jin Y-T, Tsai T, Shiau A-L, Wu C-L, Su W-c. Constitutive activation of Stat3 and Stat5 is present in majority of nasopharyngeal carcinoma and correlates with better prognosis. Britich J Cancer 2003;89:344–9.
18. Boise LH, Gonzalez-Garcia M, Postema CE, et al. Bcl-x, a bcl-2-related gene that functions as a dominant regulator of apoptotic cell death. Cell 1993;74:597–608.
19. Zhou P, Qian L, Kozopas KM, Craig RW. Mcl-1, a bcl-2 family member, delays the death of hematopoietic cells under a variety of apoptosis-inducing conditions. Blood 1997;89:630–43.
20. Grandis JR, Drenning SD, Chakraborty A, et al. "Requirement of Stat3 but not Stat1 activation for epidermal growth factor receptor- mediated cell growth in vitro." J Clin Invest 1998;102:1385–92.
21. Grandis JR, Drenning SD, Zeng Q, et al. Constitutive activation of stat3 signaling abrogates apoptosis in squamous cell carcinogenesis in vivo. Proc Natl Acad Sci USA 2000;97:4227–32.
22. Barton BE, Karras JG, Murphy TF, Barton A, Huang HF-S. signal transducer and activatior of transcription 3 (STAT3) activation in prostate cancer: direct Stat3 inhibition induces apoptosis in prostate cancer lines. Mol Cancer Ther 2004;3:11–20.
23. Leong PL, Andrews GA, Johnson DE, et al. targeted inhibition of Stat3 with a decoy oligonucleotide abrogates head and neck cancer cell growth. Proc Natl Acad Sci USA 2003;97:4138–43.
24. Burdelya L, Catlett-Falcone R, Levitzki A, et al. Combination therapy with AG-490 and interleukin 12 achieves greater antitumor effects than either agent alone. Mol Cancer Therapeutics 2002;1:893–9.
25. Blaskovich MA, Sun J, Cantor A, Turkson J, Jove R, Sebti SM. Discovery of JSI-124 (Cucurbitacin I), a selective janus kinase/signal transducer and activitor of transcription 3 signaling pathway inhibitor with potent antitumor activity against human and murine cancer cells in mice. Cancer Res 2003;63:1270–9.
26. Becker S, Groner B, Muller C. Three-dimensional structure of the Stat3β homodimer bound to DNA. Nature 1998;394:145–50.
27. Jing N, Li Y, Xu X, Li P, Feng L, Tweardy D. Targeting Stat3 with G-quartet oligonucleotides in human cancer cells. DNA Cell Biol 2003;22:685–96.
28. Williamson JR. G-quartet structures in telomeric DNA. Annu Rev Biophys Biomol Structure 1994;23:703–30.
29. Gilber DE, Feigon J. Multistranded DNA structures. Current Opinion Structura Biol 1999;9:305–14.
30. Sen D, Gilbert W. Formation of parallel four-stranded complexes by guanine-rich motif for meiosis. Nature 1998;334:364–6.
31. Bock LC, Griffin LC, Latham JA, Vermaas EH, Toole JJ. Selection of single-stranded DNA molecules that bind and inhibit human thrombin. Nature 1992;355:564–6.
32. Wyatt JR, Vickers TA, Roberson JL, et al. Combinatorially selected guanosine-quartet structure is a potent inhibitor of HIV envelope-mediated cell fusion. Proc Natl Acad Sci USA 1994;91:1356–60.
33. Rando RF, Ojwang J, Elbaggari A, et al. Suppression of human immunodeficiency virus type 1 activity in vitro by oligonucleotides which form intramolecular tetrads. J Biol Chem 1995;270:1754–60.
34. Mazumder A, Neamati N, Ojwang JO, Sunder S, Rando RF, Pommier Y. Inhibition of the human immunodeficiency virus type 1 integrase by guanosine quartet structures. Biochemistry 1996;35:13762–71.
35. Jing N, De Clercq E, Rando FR, et al. Stability-activity relationships of a family of G-tetrad forming oligonucleotides as potent HIV inhibitors. J Biol Chem 2000;275: 3421–30.
36. Marchand C, Pourquier P, Laco GS, Jing N, Pommier Y. Interaction of human nuclear topoisomerase I with guanosine quartet-forming and guanosine-rich single-stranded DNA and RNA oligonucleotides. J Biol Chem 2002;277:8906–11.
37. Xu X, Hamhouyia F, Thomas SD, et al. Inhibition of DNA replication and induction of —phase cell cycle arrest by G-rich oligonucleotides. J Biol Chem 2001;276: 43221–30.
38. Schreiber WE, Jamani A. Pudek MR. Screening tests for porphobilinogen are insensitive. The problem and its solution. Am J Clin Pathol 1989;92:644–9.
39. Jing N, Hogan ME. Structure-activity of tetrad-forming oligonucleotides as a potent anti-HIV therapeutic drug. J Biol Chem 1998;273:34992–9.
40. Jing N, Xiong W, Guan Y, Pallansch L, Wang S. Potassium dependent folding: a key to intracellular delivery of G-quartet oligonucleotides as HIV inhibitors. Biochemistry 2002;41:5397–403.
41. Bishop JS, Guy-Caffey JK, Ojwang JO, et al. G-quartet motifs confer nuclease resistance to a potent anti-HIV oligonucleotide. J Biol Chem 1996;271:5698–703.
42. O'Shea JJ, Gadina M, Schreiber RD. Cytokine signaling in 2002: new surprises in the Jak/Stat pathway. Cell 2002;109, Suppl:S121–31.
43. Chen X, Vinkemeier U, Zhao Y, Jeruzalmi D, Darnell JE, Kuriyan J. Crystal structure of a tyrosine phosphorylated Stat-1 dimer bound to DNA. Cell 1998;93:827–39.
44. Wiederkehr-Adam M, Ernst P, Muller K, et al. Characterization of phosphopeptide motifs specific for the Src homology 2 domains of signal transducer and activator of transcription 1 (STAT1) and STAT3. J Biol Chem 2003;278:16117–28.
45. Wallace TL, Gamba-Vitalo C, Loveday KS, Cossum PA. Acute, multipe-dose, and genetic toxicology of AR177, an anti-HIV oligonucleotide. Toxicol Sci 2000;53:63–70.
46. Schendel SL, Xie Z, Montal MO, Matsuyama S, Montal M, Reed JC. Channel formation by antiapoptotic protein Bcl-2. Proc Natl Acad Sci USA 1997;94:5113–8.
47. Minn AJ, Velez P, Schendel SL, et al. Bcl-x(L) forms an ion channel in synthetic lipid membranes. Nature 1997;385:353–7.